Transworld Research Network
37/661 (2), Fort P.O., Trivandrum-695 023, Kerala, India


Nanoscale Interactions and Their Applications: Essays in Honour of Ian McCarthy, 2007: 79-93 ISBN: 81-7895-255-6 Editors: Feng Wang and Michael J. Brunger

# 8 Coupled channels and planetary atmospheres

**B. R. Lewis, S. T. Gibson and A. N. Heays**
Research School of Physical Sciences and Engineering, The Australian National University, Canberra, ACT 0200, Australia

## Abstract

*An outline is given of the application of radial coupled channels techniques to the problem of diatomic molecular photodissociation. Specific coupled-channel calculations of photodissociation cross sections are performed for diatomic sulphur and nitrogen, of importance in understanding the photochemical and radiative behaviours of the atmospheres of Io and Titan, respectively.*

Correspondence/Reprint request: Prof. B. R. Lewis, Research School of Physical Sciences and Engineering The Australian National University, Canberra, ACT 0200, Australia. E-mail: brl121@rsphy1.anu.edu.au

provide partial cross sections, dissociation branching ratios, predissociation quantum yields, and seamless isotopic information. Due to these characteristics, CC models of diatomic molecular spectroscopy and dissociation dynamics are expected to find wide applicability in the analysis of data from planetary-atmospheric missions.

## Acknowledgement

This research was supported under the Australian Research Council's Discovery funding scheme (project number DP0558962).

## References

1. McCarthy, I. E. and Stelbovics, A. T. 1983, Phys. Rev. A, 28, 2693.
2. McCarthy, I. E. and Stelbovics, A. T. 1983, J. Phys. B, 16, 1233.
3. Bartlett, P. L., Williams, J. F., Bray, I., Mikosa, A. G., and Stelbovics, A. T. 2006, Phys. Rev. A, 74, 022714.
4. Mies, F. H. 1980, Molec. Phys., 41, 953.
5. van Dishoeck, E. F., van Hemert, M. C., Allison, A. C., and Dalgarno, A. 1984, J. Chem. Phys., 81, 5709.
6. Noll, K. S., McGrath, M. A., Trafton, L. M., Atreya, S. K., Caldwell, J. J., Weaver, H. A., Yelle, R. V., Barnet, C., and Edgington, S. 1995, Science, 267, 1307.
7. Spencer, J. R., Jessup, K. L., McGrath, M. A., Ballester, G. E., and Yelle, R. 2000, Science, 288, 1208.
8. Torop, L., McCoy, D. G., Blake, A. J.,Wang, J., and Scholz, T. 1987, J. Quant. Spectrosc. Radiat. Transfer, 38, 9.
9. Lefebvre-Brion, H. and Field, R. W. 2004, The spectra and dynamics of diatomic molecules, Elsevier, Amsterdam.
10. Gibson, N. D., Kortshagen, U., and Lawler, J. E. 1996, J. Appl. Phys., 79, 7523.
11. Leone, S. R. and Kosnik, K. G. 1997, Appl. Phys. Lett., 30, 346.
12. Wheeler, M. D., Newman, S. M., and Orr-Ewing, A. J. 1998, J. Chem. Phys., 108, 6594.
13. Green, M. E., and Western C. M. 1996, J. Chem. Phys., 104, 848.
14. Lewis, B. R., Gibson, S. T., Hawes, F. T., and Torop, L.W. 2001, Phys. Chem. Earth C, 26, 519.
15. Pradhan, A. D. and Partridge, H. 1996, Chem. Phys. Lett, 255, 163.
16. Dressler, K. 1969, Can. J. Phys., 47, 547.
17. Carroll, P. K. and Collins, C. P. 1969, Can. J. Phys., 47, 563.
18. Lefebvre-Brion, H. 1969, Can. J. Phys., 47, 541.
19. Stahel, D., Leoni, M., and Dressler, K. 1983, J. Chem. Phys., 79, 2541.
20. Lewis, B. R., Gibson, S. T., Zhang,W., Lefebvre-Brion, H., and Robbe, J.-M. 2005, J. Chem. Phys., 122, 144302.
21. Haverd, V. E., Lewis, B. R., and Gibson, S. T. 2005, J. Chem. Phys., 123, 214304.
22. Spelsberg, D. and Meyer, W. 2001, J. Chem. Phys., 115, 6438.
23. Sprengers, J. P., Ubachs, W., Baldwin, K. G. H., Lewis, B. R., and Tchang-Brillet, W.- Ü 2003, J. Chem. Phys., 119, 3160.
24. Sprengers, J. P. and Ubachs, W. 2006, J. Molec. Spectrosc., 235, 176.



estimates which must be optimised by comparison between the CC-model results and the experimental database.

The radial CC method holds many advantages over conventional techniques when employed to provide information on molecular structure and photodissociation dynamics for use in the radiative and photochemical modelling of planetary atmospheres. First, partial cross sections for dissociation into the various molecular dissociation limits are a natural result of the CC method. Thus, information on dissociation branching ratios and the kinetic and internal energies of the atomic dissociation products is readily available. This information is of particular significance to the photochemical modelling of planetary atmospheres. Second, once the electronic model parameters have been ascertained, isotopic CC computations may be performed simply by changing the molecular mass appropriately. Isotopic fractionation mechanisms are a hot topic in planetary-atmospheric science and the contribution of photodissociation to these processes has been under-investigated. Third, since the radial CC model is a physically-based quantum-mechanical model, it has great predictive power when compared with conventional spectroscopic models. This is extremely important considering that it is impossible to take experimental data over a sufficient range of pressures, temperatures, energies, and isotopomers to obviate the need for interpolation and extrapolation.

In this work, we describe the formulation of a radial CC model for the computation of diatomic molecular photodissociation cross sections and discuss two applications of relevance to planetary-atmospheric studies. First, predissociation in the $B^3\Sigma_u^-$ state of $S_2$ is treated. This is of importance to studies of the atmospheres of Jupiter and Io, where absorption due to the $B^3\Sigma_u^- - X^3\Sigma_g^-$ transition has been observed [6, 7]. Finally, isotopic effects in the photodissociation of $N_2$ *via* the $c'^1\Sigma_u^+$ state are discussed. This is of timely significance to studies of the atmosphere of Titan, which has recently been visited by the *Cassini* mission.

## Theoretical method

### Coupled-channel formalism

The diatomic-molecular CC approach employed here, formulated in the diabatic basis, has been detailed by [5] and [8]. Briefly, the partial cross section for photodissociation from the $v''$, $J''$ rovibrational level of an initial uncoupled electronic state $\Phi_i$, into the energy-$E$, $J$ rotational level of a given open (dissociative) channel $o$, which is one of a total of $n$ coupled channels (each associated with an electronic state $\Phi_k$), $n_o$ of which are open, is given by

starlight by the interstellar medium [27], corresponding to the first interstellar detection of $N_2$.

In Fig. 6, the computed CC rotational dependence of the $c' - X(0, 0)$ band oscillator strength for $^{14}N_2$ is compared with the experimental results of Stark *et al.* [25], with generally excellent agreement. In particular, both experiment and theory show evidence of perturbation by other electronic states. At $J' = 10$, a sharp drop in both the experimental and CC oscillator strengths (and an accompanying shift in energy levels) reveals a nearly degenerate level crossing and resultant Rydberg-valence mixing between $c'\,^1\Sigma_u^+(v = 0)$ and $b'\,^1\Sigma_u^+(v = 1)$. A quantum interference effect due to rotational mixing of the $^1\Pi_u - X$ and $^1\Sigma_u^+ - X$ transition moments [9] is revealed by the divergence in the $P$- and $R$-branch oscillator strengths with increasing rotation. The reversal of the differentiation of the CC-model strengths near $J = 23$ indicates a further level crossing with a $^1\Pi_u$ state, namely $b(v = 5)$.

The $c'(v = 0)$ level widths and predissociation rates vary with isotopomer and rotation. An understanding of this dependency is of particular importance in explaining the heavy-isotopic enrichment detected in the $N_2$ atmosphere of Titan, which exhibits a 4.5 times greater $^{15}N$:$^{14}N$ ratio than on the Earth [28]. Because atomic escape is a driving process behind this enrichment [29], details

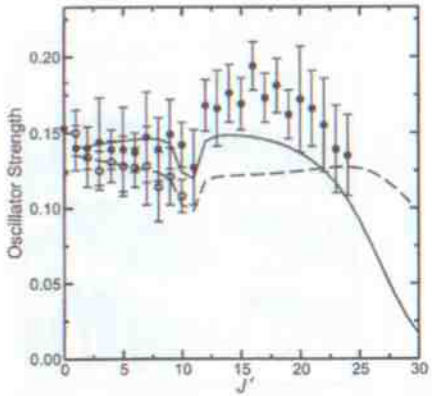


**Figure 6.** Rotational dependence of oscillator strength for the $c'\,^1\Sigma_u^+ - X\,^1\Sigma_u^+$ (0, 0) band of $^{14}N_2$. Filled and open circles represent the $P$- and $R$-branch experimental results of [25]. Solid and dashed lines, respectively, represent the corresponding CC-model values.



$\langle \Phi_k | \mathbf{H}^{el} + \mathbf{H}^{rot} + \mathbf{H}^{so} | \Phi_j \rangle$, containing, in general, the effects of electrostatic, rotational and spin-orbit interactions.

If the electronic wavefunctions are expressed in the Hund's case (a) *e/f* parity basis [9], then the only non-zero elements of $D(R)$ arise from dipole-allowed parallel and perpendicular transitions between case (a) basis states. In the case of a finite temperature $T$, the partial or total photodissociation cross sections can be expressed as sums of cross sections into the upper-state levels of $e$ and $f$ parity, each of which is calculated separately as a Boltzmann sum of Eqs. (1) or (4), respectively, over the initial distribution of levels. Thus, the partial cross section for photodissociation into open channel $o$ becomes:

$$\sigma_{oE \leftarrow iT} = \sum_{v'',J'',p''} \sum_{J,p} \alpha_{iTv''J''p''} \sigma_{oEJp \leftarrow iv''J''p''}, \tag{6}$$

and the total cross section is given by

$$\sigma_{E \leftarrow iT} = \sum_{v'',J'',p''} \sum_{J,p} \alpha_{iTv''J''p''} \sigma_{EJp \leftarrow iv''J''p''}, \tag{7}$$

where the $\alpha_{iT,v''J''p''}$ are appropriately weighted statistical-Boltzmann factors for the initial levels, and $p$ and $p''$ have two possible values, $e$ and $f$.

## Results and discussion

### $S_2$

The $B^3\Sigma_u^- - X^3\Sigma_g^-$ transition of $S_2$, which consists of a series of well-separated $(v', 0)$ bands in the 250–290 nm region, has been observed in absorption in the atmospheres of Jupiter and Io [6, 7]. This transition, in emission, is responsible for the efficient production of visible light from microwave-powered sulphur lamps [10] and has also been identified for possible laser applications [11].

The occurrence of isolated $S_2$ is uncommon, except under exotic circumstances such as in high-temperature vapours or sulphur-containing flames and discharges. Therefore, there has been only limited experimental investigation of the $B - X$ photoabsorption spectrum of $S_2$. However, this transition is known to exhibit an interesting spectral dichotomy, where the vibrational bands below $v' = 9$ are more readily observed in emission, while the higher vibrational bands are seen in absorption and are substantially diffuse [12, 13]. This behaviour reflects the onset of a complex predissociation mechanism.

is extended by the inclusion of three additional homogeneously interacting $^1\Sigma_u^+$ states and their accompanying rotational coupling to the $^1\Pi_u$ manifold, allowing, for the first time, the calculation of *e*-parity rovibrational cross sections which include the effects of predissociation.

The diabatic $\Pi_u$ PECs, couplings, and electronic transition moments employed in the current CC model are taken from [20] and [21]. In the case of the $^1\Sigma_u^+$ states, the *ab initio* and fitted polynomial PECs of [22] were employed as a starting point and further optimised semiempirically by a least-squares fitting routine associated with the CC model. Significant improvements have been made possible by comparison with a larger experimental database, including measurements on the $^{14}N^{15}N$ and $^{15}N_2$ isotopomers [23, 24]. The optimized $^1\Sigma_u^+$ PECs employed in the current CC model are those shown in Fig. 4. The electronic coupling functions between the $^1\Sigma_u^+$ states are $R$ dependent [22]. Our $V_{b'c'}$ $(R)$ was taken from [22] and scaled during the optimisation of energy levels by a factor of 0.98. In the representation chosen for this model, the diabatic coupling $V_{c'c'}$ is set to zero and the radial dependency of $V_{b'c'}$ is the same as that of $V_{b'c'}$, but scaled by 0.49, as appropriate for members of a Rydberg series. $R$-independent parameters have been used to rotationally couple the $^1\Sigma_u^+$ and $^1\Pi_u$ *e*-parity states with fitted values of $V_{b'b} = -0.2$ cm$^{-1}$, $V_{c'c} = 2.00$ cm$^{-1}$ and $V_{b'o} = -0.62$ cm$^{-1}$, all with an

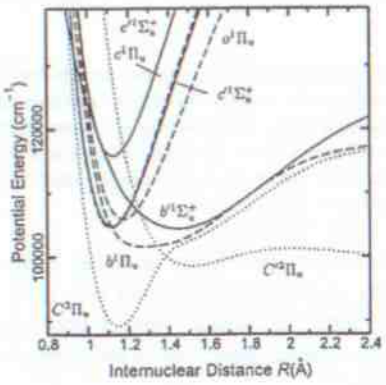


**Figure 4.** Relevant excited-state potential energy curves of $N_2$, shown in a diabatic representation. The energy scale is referred to the minimum in the $X^1\Sigma_g^+$ ground-state potential (not shown).



Only the $B^3\Sigma_u^-$ and $B''\ ^3\Pi_u$ states have optically allowed transitions from the $X^3\Sigma_g^-$ ground state. The ab initio curves [15] for these electronic transition moments are shown as an inset in Fig. 1, and illustrate that the $B'' - X$ transition is substantially weaker than the $B - X$ transition.

As noted above, predissociation of the $B^3\Sigma_u^-$ state occurs through coupling to the dissociative states. The spin-orbit ($\Delta\Omega = 0$) coupling constants employed in the present CC model, assumed to be $R$-independent, are 60 cm$^{-1}$, 100 cm$^{-1}$, and 90 cm$^{-1}$, for the $B \sim B''$, $B \sim {}^5\Pi_u$, and $B \sim {}^1\Pi_u$ interactions, respectively. The $2\,^3\Sigma_u^+$ state predissociates only the high-$v'$ levels of the $B^3\Sigma_u^-$ state and has not been included in this model calculation. Rotational coupling ($\Delta\Omega = \pm 1$) occurs between the $^3\Sigma_{1e}^-$ and $^3\Sigma_{0e}^-$ states. In the ground state, $X^3\Sigma_g^-$, fine-structure splittings arise from the 445 cm$^{-1}$ spin-orbit interation [9] between the $^3\Sigma_0^-$ substate and the metastable $b^1\Sigma_0^+$ state, together with a small rotational coupling between the ground-state sublevels of *e* parity. The rotational-branch structure is identical to that of $O_2$, with fourteen distinct branches. However, due to the diffuse nature of the $S_2$ bands, in the present CC calculation, for simplicity, only the six strong $P$ and $R$ branches have been included.

Computed CC partial cross sections are shown in Fig. 2 for the *f*-parity manifold. These cross sections illustrate the complex and varying roles of each

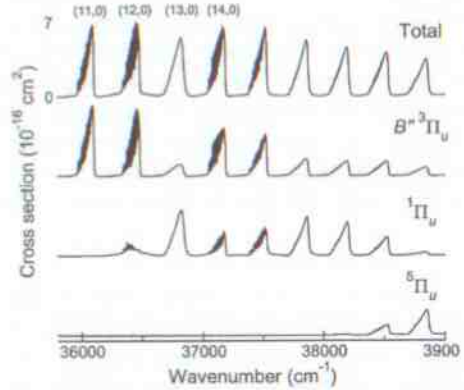


**Figure 2.** Computed CC cross section for the *f*-parity rotational levels of the $B - X$ system of $S_2$ at $T = 300$ K. Partial cross sections to each dissociating state are also shown. Predissociation is initiated by $B''^3\Pi_u$, followed by $^1\Pi_u$ and $^5\Pi_u$, as dissociation *via* these states becomes energetically accessible.

of the predissociating states. Predissociation is initiated by the $B''^3\Pi_u$ state, near $v' = 11$, once this dissociation channel is energetically available. The other continuum states contribute for the higher-$v'$ bands. In contrast to the conclusions of Wheeler *et al.* [12], it is seen that the $B''^3\Pi_u$ state does make a substantial contribution to many bands. In general, the appearance of rotational structure is lost through the strong predissociation broadening. This aspect is most evident for the (13,0) band, in comparison with adjacent bands. Unlike line-by-line band models, the CC model correctly predicts the cross section between resonances, implicitly characterizing the interference between bound levels and continua. A complex interaction between rovibrational transitions into the $B$-state with the underlying pseudocontinuum results in a variety of line shapes and asymmetries.

The total cross section is obtained by adding the contributions from the $f$– and $e$-parity manifolds. Room-temperature total CC cross sections for the (11,0) to (14,0) $B$–$X$ bands are shown in Fig. 3, together with the experimental cavity-ring-down measurements of Wheeler *et al.* [12]. The CC calculations demonstrate qualitative agreement with the measurements, reproducing the shoulder at the band-head, resulting from the fine-structure splitting of the ground state, and also the observed trend in rovibrational linewidths. This aspect is most evident for the (13,0) band, where the apparent rotational structure is diminished due to the influence of predissociation by the $^1\Pi_u$ state.

In summary, application of the CC model to the $B - X$ transition of $S_2$ clearly identifies the role of each predissociating state, which is essential to understanding the complexities of the spectrum. The CC cross sections agree well in shape with the published spectra [12]. However, the experimental data is limited and not calibrated in magnitude. Following the availablity of further experimental data, improvements to the CC model may be achieved through adjustment of the CC-model parameters, in particular, the PECs for the dissociative states, their spin-orbit couplings to the $B$ state, and the $B - X$ transition moment Also, extending the calculations to the lower-$v'$ bands, which have narrow structures, will provide a more detailed comparison.

## $N_2$

The electronic spectrum of molecular nitrogen has been studied extensively, but its successful interpretation in the EUV region proved elusive until the simultaneous studies of three authors [16, 17, 18] showed that the chaotic behaviour of the spectrum in this region could be explained within a framework of strong Rydberg-valence interactions involving states of $^1\Pi_u$ and $^1\Sigma_u^+$ symmetries. These interactions were first treated quantitatively in a benchmark paper by Stahel *et al.* [19]. PECs for the relevant excited electronic states of $N_2$ are shown in Fig. 4. Recently, it has been shown that the



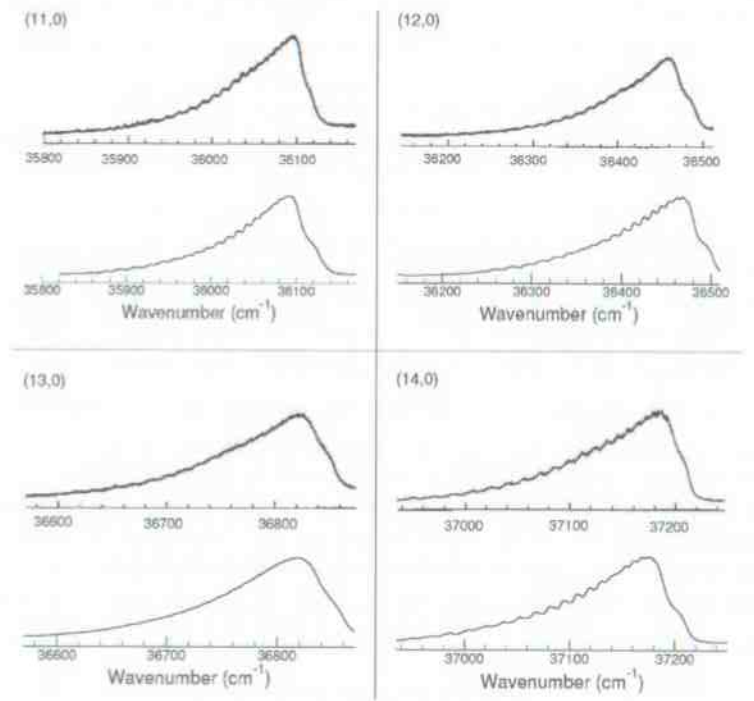


**Figure 3.** $S_2$ total photodissociation cross sections in arbitrary units. Upper curves in each block: Room-temperature cavity-ring-down spectroscopic measurements of Wheeler *et al.* [12]. Lower curves : Comparable CC computations of this work. The shoulder at the band-head arises from the fine-structure splitting in the ground state. The appearance of rotational structure in the (13,0) band is diminished due to the influence of predissociation by the $^1\Pi_u$ state.

significant and haphazard predissociation observed in the lowest $^1\Pi_u$ states of $N_2$ is caused indirectly, through an additional spin-orbit coupling to the $^3\Pi_u$ manifold, involving both the bound valence-hole state, $C^3\Pi_u$, and the continuum of the $C''^3\Pi_u$ valence state, which are themselves coupled strongly [20].

In [20] and [21], a CC model of $N_2$ $f$-parity singlet and triplet $\Pi_u$ states was implemented. This model has been used to explain the energy perturbations and widths of the lowest-energy $^1\Pi_u$ levels, together with the corresponding $^1\Pi_u - X^1\Sigma_g^+$ $(v', 0)$ oscillator strengths. Here, the model of [20]

$S_2$ is isovalent with $O_2$, in which the analogous $B$–$X$ spectrum, the Schumann-Runge system, has been extensively studied both experimentally and theoretically. In particular, detailed aspects of the $O_2$ photodissociation spectrum are well described by a CC model [14]. Here, a similar CC model is applied to the $B$–$X$ transition of $S_2$. This model provides considerable insight into the nature of the spectrum, revealing the predissociation mechanisms that lead to line broadening and predicting the detailed shape of the $S_2$ photoabsorption spectrum.

Relevant electronic PECs for $S_2$ are shown in Fig. 1. Strong photoabsorption occurs from the $X\,^3\Sigma_g^-$ ground state to the $2\,^3\Sigma_u^+$ state, which, as for the $B$ state of $O_2$, is predissociated by the $^3\Pi_u$, $^5\Pi_u$, $^1\Pi_u$ and $2\,^3\Sigma_u^+$ states. The $^5\Sigma_u^-$ state employed by Wheeler *et al.* [12] is forbidden to interact with $B\,^3\Sigma_u^-$ [9]. The $X\,^3\Sigma_g^-$, $B''\,^3\Pi_u$, and $B\,^3\Sigma_u^-$ PECs shown in Fig. 1 and employed in the CC model are Rydberg-Klein-Rees curves derived from published spectroscopic constants [13], while the $^1\Pi_u$, $^5\Pi_u$, and $2\,^3\Sigma_u^+$ PECs are from *ab initio* calculations [12], shifted to the correct dissociation limit.

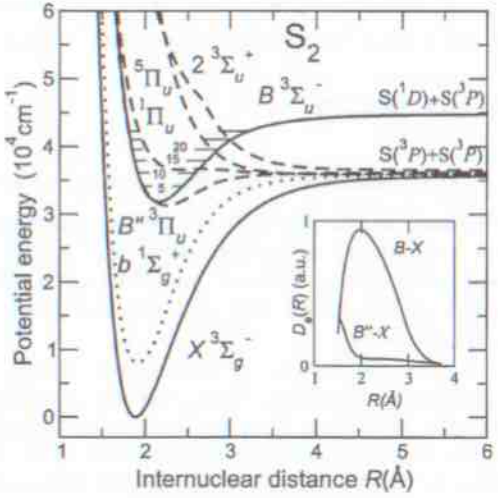


**Figure 1.** Potential-energy curves of $S_2$ relevant to the $B$–$X$ study. The $B$ state (solid curve) is predissociated first by the $^3\Pi_u$, $^1\Pi_u$, and $^5\Pi_u$ states (dashed curves). The optically-allowed electronic transition moments are shown in the inset.



additional $\sqrt{J(J+1)}$ dependence. Model $^1\Sigma_u^+ - X\,^1\Sigma_g^+$ electronic transition moments, $D(R)$, were optimised to reproduce the rotationally-resolved absolute oscillator strength measurements of [25]. The transition moments of [22] were employed for the $b' - X$ and $c' - X$ transitions, after being scaled in magnitude by factors of 0.91 and 0.83, respectively. A reversal in sign, relative to the $^1\Pi_u$ block, was also necessary to account correctly for the phase of the observed $P$- and $R$-branch quantum interference in intensity caused by the rotational interactions with the $^1\Pi_u$ states [9].

The strongest band in the entire dipole-allowed absorption spectrum of $N_2$ arises from the Rydberg transition $c'\,^1\Sigma_u^+ - X\,^1\Sigma_g^+$ (0,0) which has been studied in some detail [26]. In an uncoupled picture, this band is strong because the $c'$-state PEC has nearly the same equilibrium internuclear separation as the ground state, resulting in a large vibrational overlap. CC-model photodissociation cross sections, calculated for $T = 300$ K in the region of $c' - X(0, 0)$ for the three isotopomers of $N_2$, are shown in Fig. 5, where, for clarity, each spectrum has been convolved with a Gaussian function of 1 $cm^{-1}$ full-width at half-maximum, since the $c'(v = 0)$ predissociation line widths are extremely narrow. This band shows little isotope shift, unlike the neighbouring band $c\,^1\Pi_u - X\,^1\Sigma_g^+(0,0)$, and is only gradually red-degraded, revealing a double-peaked structure at low resolution, corresponding to the $P$ and $R$ branches. Such a structure has been recorded recently in the absorption of

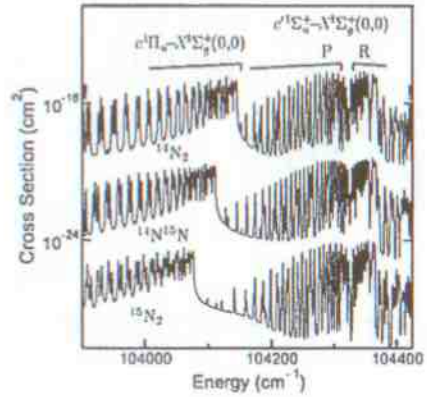


**Figure 5.** CC-model photodissociation cross sections for the isotopomers of $N_2$ at $T =$ 300 K. For clarity, the $^{14}N^{15}N$ and $^{15}N_2$ results have been reduced by factors of $10^{-5}$ and $10^{-10}$, respectively.

$$\sigma_{oEJp\leftarrow iv''J''p''} = 1.23\times10^{-23} g\nu \left|\langle \chi_{oEJp}(R)\,|\mathbf{M}(R)|\,\chi_{iv''J''p''}(R)\rangle\right|^2 \text{ cm}^2, \quad (1)$$

where $p''$ and $p$ represent the parities of the initial and final levels, respectively, $\nu$ is the transition energy in $\text{cm}^{-1}$, the degeneracy factor $g = (2-\delta_{0,\Lambda'+\Lambda''})/(2-\delta_{0,\Lambda''})$, and the transition matrix elements are in atomic units. $\chi_{oEJp}(R)$ is the $n \times 1$ coupled-channel radial wavefunction vector for the open channel $o$. $\chi_{Jv''J''p''}(R)$ is the radial wavefunction of the initial state and the elements of the $n\times1$ rotronic transition moment vector $\mathbf{M}(R)$ are the products of appropriately normalized electronic transition moments and rotational matrix elements, $M_k(R) = D_{ki}(R)A_k$, where the elements of the electronic transition moment vector $\mathbf{D}(R)$ are

$$D_{ki}(R) = \langle \Phi_k\,|\mu|\,\Phi_i\rangle\,, \quad (2)$$

and the purely rotational matrix elements

$$A_k = \langle J\Omega_k\,|\alpha_Z|\,J''\Omega''\rangle\,, \quad (3)$$

where $\mu$ and $\alpha_Z$ are the electric dipole and direction-cosine operators, respectively. The total parity- and rovibration-specific photodissociation cross section into all open channels is given by

$$\sigma_{EJp\leftarrow iv''J''p''} = \sum_o \sigma_{oEJp\leftarrow iv''J''p''}\,. \quad (4)$$

The $n \times n_o$ coupled-channel radial wavefunction matrix $\chi_{EJp}(R)$, consisting of the set of column vectors $\chi_{oEJp}(R)$, is given by the solution of the diabatic-basis coupled Schrödinger equations, expressed in matrix form,

$$\left\{\mathbf{I}\frac{d^2}{dR^2} + \frac{2\mu}{\hbar^2}\left[E\mathbf{I} - \mathbf{V}(R) - \mathbf{V}^{\text{rot}}(R)\right]\right\}\chi_{EJp}(R) = 0, \quad (5)$$

where $\mu$ is the molecular reduced mass, $R$ is the internuclear separation, and $\mathbf{I}$ is the identity matrix. $\mathbf{V}(R)$, of dimension $n \times n$, is the symmetric diabatic potential matrix, the diagonal elements of which are the diabatic electronic potential energy curves $V_k(R) = \langle \Phi_k\,|\mathbf{H}^{\text{el}}|\,\Phi_k\rangle$, and $\mathbf{V}^{\text{rot}}(R)$ is a diagonal matrix with elements $V^{\text{rot}}_{kk}(R) = \langle \Phi_k\,|\mathbf{H}^{\text{rot}}|\,\Phi_k\rangle$, where $\mathbf{H}^{\text{rot}}$ is the rotational part of the molecular Hamiltonian. The couplings between the interacting electronic states are given by the off-diagonal elements of $\mathbf{V}(R)$, $V_{kj}(R) =$



of the EUV absorption and electron excitation cross sections for the $c'(v=0)$ state, and the relative importances of its radiative and predissociative decay mechanisms, are required. The CC-model results of Fig. 7 show significant rotational and isotopic dependences in the predissociation yield. The initial increase in the $^{14}N_2$ predissociation yield with rotation is due to increased rotational mixing between $c'\,^1\Sigma_u^+(v=0)$ and $c'^1\Pi_u\,(v=0)$, leading indirectly to increased predissociation *via* $b^1\Pi_u$ $(v=5)$ and the $^3\Pi_u$ manifold. The decrease in CC predissociation for $J > 15$, in comparison with the experimental measurements of [26] may be due to the omission of the $^3\Pi_u$ Rydberg states $F$ and $G$ from the current model. The $F(v=0)$ level has recently been observed near 104730 $\text{cm}^{-1}$ [30], slightly higher in energy than $c'(v=0)$.

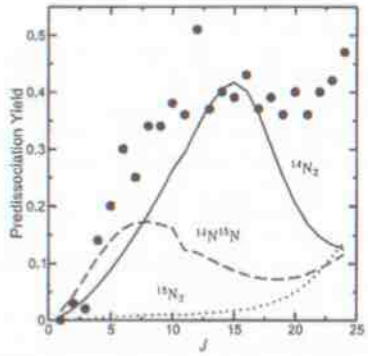


**Figure 7.** Rotational dependence of predissociation yield for the $c'\,^1\Sigma_u^+(v=0)$ state of $N_2$. Circles: Experimental results for $^{14}N_2$ from electron-impact emission study of [26] (uncertainties ±0.25). Curves: CC-model results.

## Summary and conclusions

The coupled-channel techniques of scattering theory, used so successfully over many years by Ian McCarthy to treat the problem of electron-atom scattering, have been adapted to treat the half-collision represented by diatomic molecular photodissociation, and applied to specific regions of the $S_2$ and $N_2$ spectra. As illustrated by these examples, the CC technique leads to physically-based quantum-mechanical models of molecular photodissociation with much greater flexibility and predictive powers than the line-by-line models normally used in planetary-atmospheric applications. In particular, the CC models

## Introduction

Some 23 years ago, Ian McCarthy pioneered the Flinders University effort on the application of electronic coupled-channel (CC) techniques to the theory of electron-atom scattering [1], with a first application to the problem of electron-hydrogen scattering [2]. Unprecedented accuracy has been obtained using the CC method to interpret the scattering of electrons from light atoms, and refinements of the electron-hydrogen problem are still occurring [3]. As we shall demonstrate, CC methods are also useful for the study of problems not requiring a full electronic implementation.

In comparison with atoms, molecular energy structures and dynamics are very rich, with the addition of vibrational and rotational degrees of freedom to the electronic structure, and the availability of the photodissociation mechanism for fragmentation. Molecular excited states often occur in energy regions where there are significant inter-state interactions, resulting in the breakdown of the Born-Oppenheimer (BO) approximation, which assumes separability of the electronic and nuclear motions. These excited states play important roles in the radiative and photochemical behaviours of planetary atmospheres, through their contribution to the absorption of solar radiation, most often in the vacuum ultraviolet (VUV) and extreme ultraviolet (EUV) spectral regions, and subsequent molecular dissociation.

The CC techniques of scattering theory [4] have been adapted to treat the "half-collision" represented by diatomic molecular photodissociation, specifically for the computation of cross sections in the case of BO-approximation breakdown where perturbative methods are inapplicable [5]. In contrast to the electronic case, here the Schrödinger equation for the coupled excited states is solved for the motion of the nuclei in the field of the molecular electrons, with the relevant coordinate $R$, the internuclear distance. In other words, the solutions are coupled *radial*, rather than electronic, wavefunctions. Either an *adiabatic* BO basis, in which potential-energy curves for the excited electronic states of a given symmetry exhibit avoided crossings and are coupled by the nuclear kinetic-energy operator, or a *diabatic* BO basis, where the curves are allowed to cross and interact electrostatically, may be employed. Both choices result in identical outcomes for a given basis size, but the diabatic basis is normally preferred since the corresponding electrostatic couplings generally vary only slowly with $R$. The electronic "parameters" required in order to use the radial CC method for the computation of photodissociation cross sections are the ($R$-dependent) molecular potential-energy curves (PECs), couplings, and transition moments. These may be computed *ab initio*, using, e.g., multireference configuration-interaction techniques. However, it is not possible to obtain parameters of spectroscopic accuracy using such methods, except for the sole case of $H_2$, so the *ab initio* results serve simply as initial



25. Stark, G., Huber, K. P., Yoshino, K., Smith, P. L., and Ito, K. 2005, J. Chem. Phys., 123, 214303.
26. Liu, X., Shemansky, D. E., Ciocca, M., Kanik, I., and Ajello, J. M. 2005, Astrophys. J., 623, 579.
27. Knauth, D. C., Andersson, B.-G., McClandiss, S. R., and Moos, H.W. 2004, Nature, 429, 636.
28. Marten, A., Hidayat, T., Biraut, Y., and Moreno, R. 2002, Icarus, 158, 532.
29. Lunine, J. I., Yung, Y. L., and Lorenz, R. D. 1999, Planet. Space Sci., 47, 1291.
30. Sprengers, J. P., Reinhold, E., Ubachs, W., Baldwin, K. G. H., and Lewis, B. R. 2005, J. Chem. Phys., 123, 144315.